Research Journal of Applied Sciences, Engineering and Technology 9(5): 374-379, 2015
DOI:10.19026/rjaset.9.1416
ISSN: 2040-7459; e-ISSN: 2040-7467

Submitted: September 18, 2014 Accepted: October 17, 2014 Published: February 15, 2015

Research Article

Region Descriptors to Extricate Renal Calculi by Discerning Artifacts from Ultra Sound Images

[1]M. Ranjitha and [2]G.M. Nasira
[1]Department of Information Technology, CMR Institute of Management Studies (Autonomous), Bangalore University, Bangalore,
[2]Department of Computer Science, Chikkana Government Arts College, Bharathiar University, Tirupur, India

Abstract: The study presents a new technique to identify kidney stones and differentiate it from artifacts from an ultra sound scanned image. Image analysis plays vital role in medical diagnosis. Analysing texture is a major source of discrimination in image analysis. There are situations when artifacts are mistaken for kidney stones in Medical scan using Ultra sound technique. We are proposing a new approach wherein the kidney stones are differentiated from artifacts using various shape descriptive parameters. Various descriptors like Compactness, Dispersion, Smoothness and third moment are used in our method to differentiate artifacts and stones from ultrasound images. Basic regional descriptor characterizes the geometric properties of ROI (Region of Interest) whereas Invariant moment concentrates on the density of ROI. Initially the US image is polished using a Combinational approach of noise removal and this image is taken as input for our further analysis. Pre-processing is done to minimize the occurrence of artifacts. The potential calculi are extracted and the validity is tested using the above specified parameters. Test results show convincing difference in values between Calculi and Artifact. The suggested method efficiently helped in identifying Renal Calculi from Ultra sound Images.

Keywords: Artifacts, compactness, density, dispersion, noise removal, renal calculi, smoothness, ultrasound

INTRODUCTION

Kidney stones otherwise called as Renal Calculi are becoming one of the common ailments. Calcium that is not used by the bones and muscles goes to the kidneys. In most people, the kidneys flush out the extra calcium with the rest of the urine. People who have calcium stones keep the calcium in their kidneys. Kidney stones are formed by crystal nucleation, growth and aggregation processes.

Small stones pass through the urine without any pain. But this stone becomes significant when the calcium, uric acid deposits are accumulated and when it attains a significant size. The patient will be aware of this only when this stone passes through urethra and gets stuck in the urinary tract which causes extreme pain. The blockage caused if the stone is not passed into the bladder by the peristaltic (spasmodic) action of the surrounding musculature will result in interruption of urine flow and subsequent renal damage (Coe *et al*., 1992). There are different types of kidney stones depending on its mineral components. The most common ones are Calcium oxalate, calcium phosphate, Struvite and Cystine stones. These stones may not be in its pure form. It will be the combination of many minerals. Struvite stones are found in individuals who have developed infection in urinary tract. These stones are called infection stones. It has been proposed that urine naturally contains substances that inhibit the development of large calcium oxalate crystals. Calcium oxalate kidney stones result when a normal crystallization-inhibitory system goes awry. Consistent with this assumption, studies have identified various urine components that can inhibit calcium oxalate crystal formation and/or aggregation (Nakagawa *et al*., 1983; Asplin *et al*., 1991; Shiraga *et al*., 1992; Atmani *et al*., 1996; Yamaguchi *et al*., 1993). Cystine stones are very rare and this stone formation runs in families.

PROBLEM STATEMENT

Ultrasound (US) scan is a popular scanning tool for any diagnosis. This technique is regarded as the safest and most adaptable method within the reach of common man in terms of cost. US scan is the first scan done by radiologists for any type of ailment. The complex physical interactions of the ultrasound beam with the human tissues results in some unexpected results in the

Corresponding Author: M. Ranjitha, Department of Information Technology, CMR Institute of Management Studies (Autonomous), Bangalore University, Bangalore, India

ultrasound scanned images. Though US images are adaptable and comparatively safe, there are some acoustic interferences and artifacts in images. As a result of variations in the propagation speed of sound in different tissues and due to the bending and vibrations encountered by ultrasound energy as it traverses complex anatomical structures or due to the improper registration and display of information on the image due to limitations of the transducer, receiver or other components of the imaging system, some artificial stone like foreign bodies appear in US scanned image. The magnitude of the electromagnetic energy captured in a digital image is represented by positive digital numbers. Shadowing artifact is caused by partial or total reflection or absorption of the sound energy. A much weaker signal returns from behind a strong reflector like air or sound -absorbing structure like gallstone, kidney stone etc results in shadowing, which confuses the radiologists for a stone as it is a common belief that stones cast shadows (Kamaya *et al*., 2003; Sumarsono, Year; Vincent and Anahi, 2011; Behnam *et al*., 2010; Tsuicheng *et al*., 2013). Emphysematous Pyelonephritis is a rare and serious complication of urinary tract infection with extensive necrosis and gas formation in the renal parenchyma. Most patients (90%) have diabetes mellitus and 20% have associated urinary tract obstruction (Patel *et al*., 1992; Lipset *et al*., 1997; Joseph *et al*., 1996). In Patients suffering from Pyelonephritis, tendency of air formation are more and these air bubbles can cast shadow which appears as Stones in US images. All these problems, complicates the identification of renal calculi by the radiologists from Ultra sound scanned images.

LITERATURE REVIEW

There are few literatures which describe the significant work that have been carried out in this area. Ioannis *et al*. (2006) proposed an algorithm for renal stone detection based on two types of image features contrast and target shape. Statistical characteristics of these features are considered based on the images of kidney recorded during optimization of Extracorporeal Shock Wave Lithotripsy (ESWL) (Ioannis *et al*., 2006). Sridhar (2012) has suggested an algorithm wherein Calculi are segmented and identified using intensity profile. Algorithm detects calculus based on the shadow it casts in ultrasound image. The potential region of the shadow is detected to a smaller portion of a polygon. Tamilselvi and Thangaraj (2011, 2012) have used seeded region growing method that performs segmentation and classification of kidney images with stone sizes using ultrasound kidney image for the analysis of stone and its early detection. The images have been classified as normal, stone and early stone stage by employing intensity threshold difference on segmented portions of the images to ease identification of multiple classes. Saurin *et al*. (2010) has used various content descriptive features like first and second order statistical parameters to classify different types of stones. Tamilselvi and Thangaraj (2012) had also suggested a Morphology based segmentation technique to extract the calculi present in ultrasound images. The above literatures have not discussed much on artifacts which is very crucial for the identification of stones.

PROBLEM SOLUTION

In our approach, we are introducing a new method to identify Kidney stones or Gall Stones and thereby differentiate artifacts and Calculi. The steps followed for our study is shown in Fig. 1.

Images for our study are collected from various Diagnostic centres. The raw images extracted from US Scan are initially pre-processed using a Combinational Approach of Noise Removing (CANR). Nasira and Ranjitha (2014a) had proposed a new technique of noise removing and smoothing (CANR) to remove the speckle noise and artifacts. Using this approach, maximum artifacts are removed and a clear image with only the possible calculi is obtained. In case of images with low contrast, Histogram equalization is performed to enhance the image (Nasira and Ranjitha, 2013). While pre-processing, we have ensured that the information for objective analysis is not disturbed as it is supposed to provide some imperative information for decision support and decision making. Since we have concentrated more on distinguishing Stones and Artifacts, we have extracted the ROI (Region of Interest) using cropping for image analysis. The intention of using multiple filters is to refine the image; thereby the image is populated with maximum occurrence of Calculi and least artifacts (Nasira and Ranjitha, 2014a). This is very much clear from the given Fig. 2. After thresholding, the stones and left out artifacts are displayed in Fig. 3. Our new findings are based on various regional descriptors to distinguish Calculi and Artifacts from an ultra sound medical image. This new approach helps the radiologists to reassure the results of their diagnosis. Any type of stone will have a rough surface and artifacts will be generally smooth. A region preserves the scalar measures based on its geometric properties. The simplest property is its size or area. The area of a region in the plane is defined as:

$$A(s) = \int_x \int_y I(x, y) dydx \tag{1}$$

where, I(x, y) = 1 if the pixel is within a shape, (x, y) ∈ S and 0 otherwise. In practice, integrals are approximated by summations. That is:

$$\sum_x \sum_y I(x, y) \Delta A \tag{2}$$

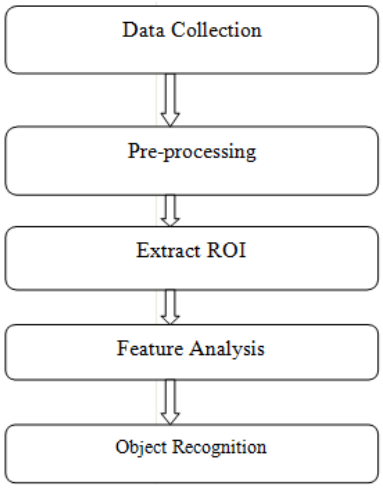

Fig. 1: Algorithm to differentiate artifacts and kidney stones

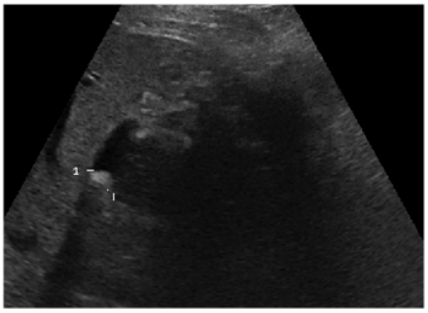

Original Image

Fig. 2: Original US image with noise and artifacts

Filtered Image Using CANR

Fig. 3: US image after applying filtering and smoothing (Using CANR algorithm)

where, ΔA is the area of one pixel. Thus, if ΔA = 1, then the area is measured in pixels. Area varies with changes in scale. One simplest property is to measure the perimeter of a region. If x (t) and y (t) denotes the parametric coordinates of a curve enclosing a region S, then the perimeter of the region is defined as:

$$P(s) = \int \sqrt{x^2(t) + y^2} \tag{3}$$

This equation represents the sums of extremely small arcs which defines the curve. x(t) and y(t) defines the set of pixels in the image. The above equation can be computed as:

$$P(s) = \sum \sqrt{(x_i - x_{i-1})^2 + (y_i - y_{i-1})^2} \tag{4}$$

where, x_i and y_i are the co ordinates of i^{th} pixel which forms the curve. Based on the above perimeter and area it is possible to describe the compactness of a region. Compactness can be measured as the ratio of perimeter to area:

$$C(S) = \frac{4\pi A(S)}{P^2(S)} \tag{5}$$

Which can be rewritten as:

$$C(S) = \frac{A(S)}{P^2(S)/4\pi} \tag{6}$$

Here, the denominator represents the area of a circle whose perimeter is P(S). Thus, compactness measures the ratio between the area of the shape and the area of the circle that can be traced with the same perimeter. That is, compactness measures the efficiency with which a boundary encloses the area. In mathematics, it is known as the isoperimetric quotient. For a perfectly circular region compactness = 1, which represents the maximum compactness value. Low values of compactness are associated with convolved regions and for elongated shapes. We are taking the advantage of this property as calculi can never be a perfect circle. Another measure that can be used to distinguish regions is dispersion. Dispersion which is otherwise called as irregularity has been measured as the ratio of major chord length to area (Chen *et al*., 1995):

$$I(S) = \frac{\pi \max((x_i - \bar{x})^2 + (y_i - \bar{y})^2)}{A(s)} \tag{7}$$

where, $(\bar{x}, \bar{y})$ denotes the coordinates of the centre of mass of the region. Numerator actually defines the area of maximum circle enclosing the region, which defines the density of the region. Another approach to measure dispersion is to calculate the ratio of maximum to minimum radius which is in fact an alternative form of irregularity (Chen *et al*., 1995):

$$IR(S) = \frac{\max(\sqrt{(x_i - \bar{x})^2 + (y_i - \bar{y})^2})}{\min(\sqrt{(x_i - \bar{x})^2 + (y_i - \bar{y})^2})} \tag{8}$$

The measure increases as the region spreads. Thus the irregularity of a circle is unity and that of a square is $\sqrt{2}$ Thus irregularity increases for irregular shapes and compactness decreases for irregular shapes. In image analysis, statistical moments plays a vital role in analyzing the texture of an image. Moments are used

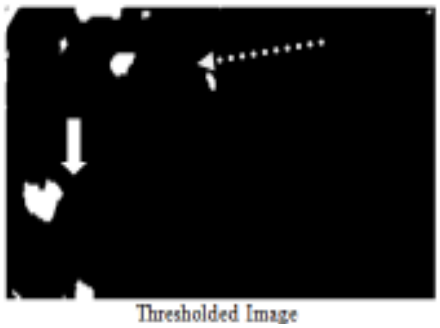

Fig. 4: Thresholded image- the thick arrow denotes a stone and dotted arrow an artifact

to portray a shape's sketch that is the arrangement of its pixels, like combining area, compactness, irregularity and higher order descriptions together. Moments are global description of a shape, accruing this same advantage. Basic regional descriptors characterises the geometric properties of the region whereas moments focus on density of the region. In our study we have taken the third order moment M3, which is an invariant descriptor and increases its value with increasing shape roughness. It reflects the asymmetry and uniformity of the histogram.

There are seven invariant moments, defined by Hu (1962), which is independent of rotation and is computed over shape boundary and its inner region (Keyes and Winstanley, 2001).

Relative smoothness, R is a measure of gray level contrast that can be used to establish descriptors of relative smoothness:

$$R = 1 - \left(\frac{1}{1 + \sigma^2} \right) \tag{9}$$

where, σ is the standard deviation of ROI. Swift variations in brightness levels reflects high spatial frequency that is roughness and crouch variations in brightness levels are related to low spatial frequencies that is smooth areas. We have exploited only those properties which show some significant differences in values for our area of study. Image analysis with its various stages of output is shown in the Fig. 2. Figure 2 is the original ultrasound scanned image of kidney. This image is filtered using CANR (Fig. 3). The possible Stones are extracted using a threshold (Fig. 4). In Fig. 4, the thick arrow denotes a stone and dotted arrow points to an artifact.

Only the possible Stone/Artifact are segmented (ROI) from the image (Fig. 3) and the above region descriptor values (Eq. 1 to 9) are computed. We have found significant changes in values of density, Compactness, dispersion, smoothness and third moment in case of stones and artifacts which is shown in Table 1 and 2 in below section.

Table 1: Experimental result of sample artifacts of US image

S. No	Compactness	Dispersion	Smoothness	Third moment
1	0.00630	57.6294	0.00068	405.400200
2	0.00270	22.9301	0.00220	2000.03000
3	0.00310	28.9204	0.00049	352.488600
4	0.00600	42.5263	0.00098	828.731300
5	0.00100	37.2580	0.00170	1202.80000
6	0.00420	63.0233	0.00056	366.149400
7	0.00740	63.4966	0.00063	380.194400
8	0.00630	32.7585	0.00100	891.075300
9	0.00410	96.7087	0.00071	649.724100
10	0.00100	74.5987	0.00240	2989.67890

Table 2: Experimental results of sample calculi of US image

S. No	Compactness	Dispersion	Smoothness	Third moment
1	0.00038	252.6855	0.00330	3602.70
2	0.00074	310.4062	0.00320	10348.00
3	0.00022	196.6209	0.01650	50586.00
4	0.00031	131.1478	0.01200	32804.00
5	0.00069	137.7044	0.00810	19082.00
6	0.00069	168.4818	0.00620	11138.00
7	0.00033	256.8434	0.00620	10947.00
8	0.00150	100.6581	0.00370	4315.300
9	0.00018	488.2154	0.00420	22680.00
10	0.00033	784.2836	0.00400	19465.00

We have already proposed in our earlier work that the density of ROI also plays a vital role in the analysis of stone and artifact (Nasira and Ranjitha, 2014b). In our earlier work we had used a statistical approach to weigh each pixel intensity according to its likelihood of being a stone or an artifact. The preprocessed image is segmented and each segment is tested for the density of the pixels in that ROI (Region of Interest) using mean. It has been observed that Mean of the probable stone is comparatively higher than the artifacts. Measuring the average value of the area gave the density of the pixels in that ROI. The Size of the stone is also computed as the total number of the pixels present in the area and multiplying the number of pixels with the dimension of one pixel (Zhou *et al*., 2001; Yang *et al*., 2004; Salman *et al*., 2005).

RESULTS AND DISCUSSION

This section presents the experimental results that are conducted in a MATLAB environment with around 30 Ultrasound images. The comparison of region descriptors like Compactness, dispersion, smoothness and third moment is shown in Fig. 5 to 8. Table 1 and 2 shows the sample test results of ten images of our experiment. It has been observed that Compactness of Artifact lies between 0.001 and 0.005 whereas for stone the range is between 0.0005 and 0.001. Low values of compactness are associated with irregular shape which is far from a perfect circle (Nixon and Aguado, 2008). Similarly, Dispersion for artifact is always less than 100 whereas for stone it was greater than 100 which entail that as irregularity (far from circle) increases dispersion also increases. Stones are not perfect circles, it has

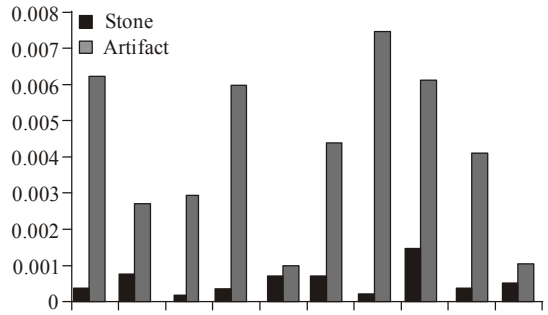

Fig. 5: Comparing compactness of stone and artifact

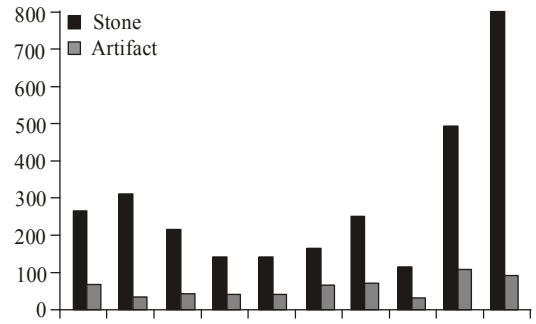

Fig. 6: Comparing dispersion of stone and artifact

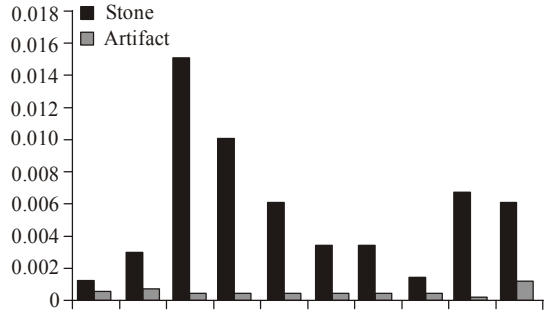

Fig. 7: Comparing smoothness of stone and artifact

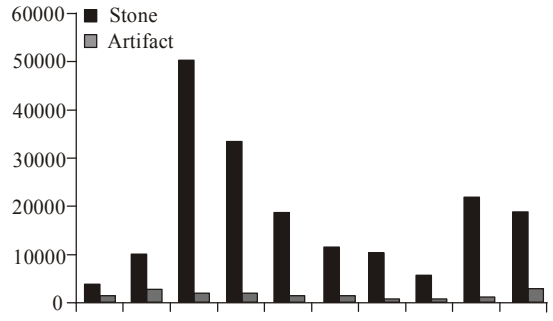

Fig. 8: Comparing third moment of stone and artifact

peaks and valleys whereas an artifact when compared to stones will be smooth and hence the dispersion values are less.

Likewise smoothness is less than 0.025 for artifacts whereas for stone it was greater than 0.025. The third moment values for artifact were within the range 300-3000 whereas it is greater than 3000 for stones. This invariant moment increases its value as the roughness increases and decreases for smooth images. It also specifies the density of ROI. Density of Stone is more than artifact. A comparison of all these parameters is presented in Fig. 5 to 8.

CONCLUSION

Objects are nothing but collection of pixels in a region which can be grouped according to some properties. From these properties, we can compare and recognize objects in an image against the values of known objects. We have introduced a new method to extract Renal/Gall stone from ultra sound Images. The proposed method also differentiates stones from artifacts by putting these two entities into two separate region categories. It can also serve as a method to distinguish the type of Stone from US images under the common assumption that Calculi stones have spikes whereas Uric acid stones are smooth. This method is based on the regional descriptors which are generally used to distinguish shapes. Depending upon the value of Compactness, dispersion, Smoothness and third moment, we have arrived at the result with fair amount of accuracy.

ACKNOWLEDGMENT

The authors would like to thank Dr. Praveen Jha of Pace Ultra Sound Centre, Bangalore, India for the guidance and for providing the images used for the study.

REFERENCES

Asplin, J., S. Deganello, Y.N. Nakagawa and F.L. Coe, 1991. Evidence that nephrocin and urine inhibit nucleation of calcium oxalate monohydrate crystals. Am. J. Physiol., 261: F824.

Atmani, F., B. Lacour and M. Daudon, 1996. Uronic acid-rich protein: A new glycoprotein inhibiting the crystallization of calcium oxalate in vitro. Nephrologie, 17: 157.

Behnam, H., A. Hajjam and H. Rakhshan, 2010. Modeling twinkling artifact in sonography. Proceeding of the 4th International Conference on Bioinformatics and Biomedical Engineering (iCBBE, 2010), pp: 1-4.

Chen, Y.Q., M.S. Nixon and D.W. Thomas, 1995. texture classification using statistical geometric features. Pattern Recogn., 28(4): 537-552.

Coe, F.L., J.H. Parks and J.R. Asplin, 1992. The pathogenesis and treatment of kidney stones. New Engl. J. Med., 327: 1141.

Hu, M.K., 1962. Visual pattern recognition by moment invariants. IEEE T. Inform. Theory, Vol. IT-8.

Ioannis, M., P. Yong-Ren, C. Chien-Chen and L. Shen-Min, 2006. Ultrasound image analysis for renal stone tracking during extracorporeal shock wave lithotripsy. Proceeding of the IEEE EMBS Annual International Conference. New York City, USA, pp: 2746-2749.

Joseph, R.C., M.A. Amendola, M.E. Artze, J. Casillas, S.Z. Jafri, P.R. Dickson and G. Morillo, 1996. Genitourinary tract gas: Imaging evaluation. Radiographics, 16(2): 295-308.

Kamaya, A., T. Tutill and J.M. Rubin, 2003. Twinkling artifact on color Doppler sonography: Dependence on machine parameters and underlying cause. Am. J. Roentgenol., 180(1): 15-22.

Keyes, L. and A. Winstanley, 2001. Using moment invariants for classifying shapes on large-scale maps. Comput. Environ. Urban, 25: 119-130.

Lipset, R.E., Kirpekar, M., K.S. Cooke and M.M. Abiri, 1997. US case of the day. Radiographics, 17: 1601-1603.

Nakagawa, Y., V. Abram, F.J. Kezdy, E.T. Kaiser and F.L. Coe, 1983. Purification and characterization of the principal inhibitor of calcium oxalate monohydrate crystal growth in human urine. J. Biol. Chem., 258: 12594.

Nasira, G.M. and M. Ranjitha, 2013. The effect of image enhancement in ultra sound kidney images. J. Res. Dev., 1(1): 1-6.

Nasira, G.M. and M. Ranjitha, 2014a. A combinational approach for noise removing and smoothing ultra sound kidney images. Int. J. Comput. Eng. Technol., 5(3): 138-147.

Nasira, G.M. and M. Ranjitha, 2014b. Proceeding of Elsevier International Conference on Advance Computing, (ICAC), pp: 132-137.

Nixon, M.S. and A.S. Aguado, 2008. Feature Extraction and Image Processing. 2nd Edn., Academic, Amsterdam, Boston, London.

Patel, N.P., R.W. Lavengood, M. Fernandes, J.N. Ward and M.P. Walzak, 1992. Gas-forming infections in genitourinary tract. Urology, 39(4): 341-345.

Salman, Y.L., M.A. Assal, A.M. Badawi, S.M. Alian and Mei-El Bayome, 2005. Validation techniques for quantitative brain tumors measurements. IEEE Proc Eng. Med. Bio., 7: 7048-7051.

Saurin, R.S., D.D. Manhar and P. Lalit, 2010. Identification of content descriptive parameters for classification of renal calculi. Int. J. Signal Image Process., 1(4): 255-259.

Shiraga, H., W. Mon, W.J. Van Dusen, M.D. Clayman, D. Miner, C.H. Terrell, J.R. Sherbotie, J.W. Foreman, C. Przysiecki and E.J. Neilson, 1992. Inhibition of calcium oxalate crystal growth in vitro by uropontin: Another member of the aspartic acid-rich protein superfamily. P. Natl. Acad. Sci. USA, 89(1): 426-430.

Sridhar, S., 2012. Segmentation of ureteric and bladder calculi in ultrasound images. J. Comput. Sci., 8(5): 716-720.

Sumarsono, Year. The Basic Principles of Ultrasonography (Usg). Chapter-14: Image Artifacts.

Tamilselvi, P.R. and P. Thangaraj, 2011. Computer aided diagnosis system for stone detection and early detection of kidney stones. J. Comput. Sci., 7(2): 250-254.

Tamilselvi, P.R. and P. Thangaraj, 2012. A modified watershed segmentation method to segment renal calculi in ultrasound kidney images. Int. J. Intell. Inform. Technol., 8(1): 46-61.

Tsuicheng, D.C., C. Sonia and F. Martin, 2013. Spin Average Supercompound Ultrasonography. Chapter 5, Intechopen.

Vincent, C. and P. Anahi, 2011. Basics of Ultrasound Imaging. Chapter 2, Atlas of Ultrasound-guided Procedures in Interventional Pain Management. Springer, New York, 2011: 13-19.

Yamaguchi, S., T. Yoshioka, M. Utsunomiya, T. Koide, M. Osafime, A. Okuyama and T. Sonoda, 1993. Heparan sulfate in the stone matrix and its inhibitory effect on calcium oxalate crystallization. Urol. Res., 21: 187.

Yang, Y., X. Yan, C. Zheng and P. Lin, 2004. A novel statistical method for segmentation of brain MRI. Proceeding of the IEEE International Conference on Communications, Circuits and Systems (ICCCAS, 2004), pp: 946-949.

Zhou, C., H.P. Chan, N. Petrick, M.A. Helvie, M.M. Goodsitt, B. Sahiner and L.M. Hadjiiski, 2001. Computerized image analysis: Estimation of breast density on mammograms. Med. Phys., 28(6): 1056-1069.